New High-Resolution Central-Upwind Schemes for Nonlinear Hyperbolic Conservation Laws

Chi-Tien Lin*

Department of Applied Mathematics, Providence University, Shalu 43301, Taiwan. *ctlin@pu.edu.tw*

Summary. The main feature of central schemes is that they are Riemann-solver free. The original high-order central scheme by Nessyahu and Tadmor [NeTa] assumes a global speed of wave propagation which introduces a large amount of numerical viscosity and lowers the resolution of discontinuities. Later, Kurganov and Tadmor [KurTa] proposed a new version of central schemes. In their construction, the whole space is divided into smooth and singular rectangular controlled volumes according to local speed of wave propagation. The updated values at each gridpoints are obtained from more precise computation on each region resulting in sharper resolution and less numerical viscosity. In this paper, we shall construct new fully-discrete central-upwind scheme by replacing the rectangular singular regions with smaller triangular regions. Numerical simulation will be present to show lower numerical viscosity and hence sharper results, as expected.

1 Introduction

Many of the modern high-resolution approximations for nonlinear conservation laws

$$\begin{cases} u_t + f(u)_x = 0 \\ u(x,t) = u_0(x) \end{cases} \tag{1}$$

employ the Godunov approach (also called the finite volume method) which consists of three consecutive steps: *reconstruction*, *evolution* and *projection*. To this end, we assume a uniform grid, $\Delta x = x_{j+1} - x_j$ for simplicity and utilize the sliding average of the solution $u(x,t)$,

$$\bar{u}(x,t) \equiv \frac{1}{|I_x|}\int_{I_x} u(s,t)ds, \qquad I_x \equiv \{s : |s-x| \leq \frac{\Delta x}{2}\}$$

so that the integration of the conservation laws (1) over the rectangle $I_x \times [t, t+\Delta t]$ yields an equivalent reformulation

$$\bar{u}(x,t+\Delta t) = \bar{u}(x,t) - \frac{1}{\Delta x}\left[\int_t^{t+\Delta t} f(u(x+\frac{\Delta x}{2},\tau))d\tau - \int_t^{t+\Delta t} f(u(x-\frac{\Delta x}{2},\tau))d\tau\right] \tag{2}$$

* This research was supported by NSC grants 88-2119-M-126-001 and 89-2115-M-126-007. Part of the work is done while the author visited the National Center of Theoretical Sciences (CTS), 18 June - 14 Sep, 2001

Assume that at time t^n, we have computed the cell average over $I_j \equiv \{x : x_{j-\frac{1}{2}} \le x \le x_{j+\frac{1}{2}}\}$, $\bar{w}_j^n$, where $x_{j+\frac{1}{2}} = (j+\frac{1}{2})\Delta x$. To compute the cell average over $I_{j+\frac{1}{2}} \equiv \{x : x_j \le x \le x_{j+1}\}$ at the next time step t^{n+1}, we first reconstruct an piecewise polynomial interpolant based on the known cell-average $\bar{w}_j^n$ at time t^n, which may result discontinuities at the points $\{x_{j+\frac{1}{2}}\}$, center of $I_{j+\frac{1}{2}}$. This interpolant is then evolved exactly in time and projected onto the cell $I_{j+\frac{1}{2}}$ at the next time level t^{n+1} according to (2), resulting with

$$\bar{w}_{j+\frac{1}{2}}^{n+1} \equiv \bar{w}(x_{j+\frac{1}{2}}, t^{n+1}) = \frac{1}{\Delta x}[\int_{x_j}^{x_{j+1}} w(x,t^n)dx - \int_{t^n}^{t^{n+1}} f(w(x_{j+1},\tau)d\tau - \int_{t^n}^{t^{n+1}} f(w(x_j,\tau)d\tau] \tag{3}$$

Here $\bar{w}(x_{j+\frac{1}{2}}, t^n)$ is the average of the interpolant $w(x,t^n)$ over the cell $I_{j+\frac{1}{2}}$. In this context, we may distinguish between the two main classes of Godunov methods, according the location of possible discontinuities: upwind and central schemes.

Godunov's original scheme is the forerunner of all upwind schemes. Its higher-order and multidimensional generalizations were constructed, analyzed, and implemented with great success during 1980s and 1990s; consult [LeVe] and the reference therein. Upwind schemes evaluate their cell averages over the same spatial cells at all time steps. This in turn requires characteristic information along the discontinuous interfaces of these spatial cells. It is the need to trace the characteristic fans– using approximate Riemann solvers, field decomposition, etc –that greatly complicates the upwind algorithms.

The Lax-Friedrichs (LxF) scheme is the other canonical first-order scheme, which is the forerunner of all central schemes. Like the Godunov scheme, it is based on piecewise constant approximate solution; its Riemann-solver-free recipe, however, is considerably simpler. Unfortunately, the excessive numerical viscosity in the LxF scheme yields a relatively poor resolution. A second-order sequel to the LxF scheme was introduced by Nessyahu and Tadmor, the Nessyahu-Tadmor (NT) scheme [NeTa] by replacing the piecewise constant approximation with van Leer's MUSCL-type piecewise linear interpolation. This is then followed by an exact evolution–LxF solver– which avoids using time-consuming approximate Riemann solver. Thus, the NT scheme retains the advantage of a simple, Riemann-solver-free recipe, and at the same time it enjoys high resolution comparable to the upwind results.

Although numerical viscosity of the second-order NT scheme is considerably lower than in the first-order LxF scheme, unfortunately, this does not circumvent the difficulties with small time steps which arise, e.g., with convection-diffusion equations. To overcome this difficulty, a new class of central schemes, *central-upwind* (KT for short) schemes, was first introduced by

Kurganov and Tadmor [KurTa]. The main idea in their construction is to use more precise information about the local speed of wave propagation, in order to average the nonsmooth parts of the computed solution over a smaller controlled rectangle of variable size of order $O(\Delta t)$. See §2.3 or [KurTa] for details. In this paper, we propose another construction. That is, to average the nonsmooth parts of the computed solution over a smaller triangular controlled volume, resulting a high resolution method with lower numerical viscosity. (See §3.)

2 LxF, NT, and KT schemes

In this section, we review briefly on the framework of central schemes for hyperbolic conservation laws (1), we shall address on the construction of the family of LxF, NT and KT schemes.

2.1 LxF schemes

The LxF approximation to (1), can be derived by constructing a piecewise-constant interpolant through the given cell-averages,

$$w(x,t^n) = \sum_j \bar{w}_j^n \chi_j(x), \tag{4}$$

whose possible discontinuities are secured at the center of the cell $\{x_j \leq \xi < x_{j+1}\}$. Here, $\chi_j(x)$ is the characteristic function over $I_j = \{x_{j-1/2} \leq \xi < x_{j+1/2}\}$. For the CFL restriction, $\Delta t \max_u |f'(u)| \leq \frac{\Delta x}{2}$, the exact solution of (1) remains constant at the integer grid points, x_{j-1}, x_j. Consequently, the required integrals of the fluxes in (3) are evaluated in terms of their constant initial data, without using any (approximate) Riemann solvers. The *staggered* LxF scheme then amounts to

$$\bar{w}_{j+\frac{1}{2}}^{n+1} = \frac{1}{2}(\bar{w}_j^n + \bar{w}_{j+1}^n) - \lambda \left[f(\bar{w}_{j+1}^n) - f(\bar{w}_j^n) \right]. \tag{5}$$

That is, we have computed an approximate solution at the next time level $t = t^{n+1}$, a solution which is realized by its cell average over $I_{j+\frac{1}{2}}$ rather than the original cell I_j. Staggered schemes may increase the difficulties in the treatment of numerical boundary conditions. However, this staggered scheme can be changed into non-staggered one by re-averaging over a piecewise constant reconstruction of the underlying staggered values $\bar{w}_{j+\frac{1}{2}}^{n+1}$ at the t^{n+1} time level, which leads to the modified LxF scheme [JLLOT],

$$\bar{w}_j^{n+1} = \frac{1}{4}(\bar{w}_{j-1}^n + 2\bar{w}_j^n + \bar{w}_{j+1}^n) - \frac{\lambda}{2} \left[f(\bar{w}_{j+1}^n) - f(\bar{w}_{j-1}^n) \right] \tag{6}$$

2.2 NT schemes

To construct the second-order NT schemes, we first reconstruct a piecewise-linear interpolant from the known cell-average $\bar{w}_j^n$ at time t^n,

$$w(x,t^n) = \sum_j [\bar{w}_j^n + (w_x)_j(\frac{x-x_j}{\Delta x})]\chi_j(x). \tag{7}$$

Here $(w_x)_j$ denotes the discrete slope. A possible computation of these slopes, which results in an overall non-oscillatory scheme, is given by the minmod limiter. (Consult [JLLOT] for others.) Note that possible discontinuities are secured at the center of the cell $I_{j+\frac{1}{2}} \equiv \{x_j < x < x_{j+1}\}$, i.e., $x_{j+\frac{1}{2}}$.

Like the construction of LxF schemes, this interpolant is then evolved in time. Under CFL restriction, the exact solution of (1) remains smooth at the integer grid points, x_{j-1}, x_j and the required integrals of the fluxes in (3) can be approximated by the midpoint rule, resulting with the staggered NT scheme,

$$\bar{w}_{j+\frac{1}{2}}^{n+1} = \frac{1}{2}(\bar{w}_j^n + \bar{w}_{j+1}^n) + \frac{1}{8}((w_x)_j - (w_x)_{j+1}) - \lambda[f(w_{j+1}^{n+\frac{1}{2}}) - f(w_j^{n+\frac{1}{2}})], \tag{8}$$

where the midpoint values, $w_j^{n+\frac{1}{2}}$, are predicted by Taylor expansion,

$$w_j^{n+\frac{1}{2}} = \bar{w}_j^n - \frac{\lambda}{2}(f_x)_j. \tag{9}$$

The discrete derivatives of the flux, $(f_x)_j$, can be computed, by the minmod limiter to each of the components of f. This component-wise approach is one of the main advantage offered by the central NT schemes over the corresponding characteristic decompositions required by upwind schemes - consult the discussion in [NeTa].

To obtain a non-staggered NT scheme, we can re-average over a piecewise linear reconstruction of the underlying staggered values, $\bar{w}_{j+\frac{1}{2}}^{n+1}$, which leads to, [JLLOT],

$$\begin{aligned}\bar{w}_j^{n+1} = \frac{1}{4}(\bar{w}_{j-1}^n + 2\bar{w}_j^n + \bar{w}_{j+1}^n) - \frac{1}{16}((w_x)_{j+1} - (w_x)_{j-1}) - \frac{\lambda}{2}[f(w_{j+1}^{n+\frac{1}{2}}) - f(w_{j-1}^{n+\frac{1}{2}})] \\ -\frac{1}{8}((w_x)_{j+\frac{1}{2}} - (w_x)_{j-\frac{1}{2}}).\end{aligned} \tag{10}$$

Here, $(w_x)_j$ and $(w_x)_{j+\frac{1}{2}}$ are, respectively, the discrete derivatives at time level t^n and t^{n+1}, and the midpoint value $w_j^{n+\frac{1}{2}}$ is predict at the time level $t^{n+\frac{1}{2}}$ according to (9).

2.3 KT schemes

The second-order NT scheme and its extensions owe their superior resolution to the lower amount of numerical dissipation, considerably lower than in the first-order LxF scheme. For problems with small time steps which arise , e.g., with convection-diffusion equations, the influence of the numerical dissipation accumulated over the many steps of the NT scheme which smears solutions. To circumvent the difficulties, a new class of central scheme was introduced by Kurganov and Tadmor, KT for short [KurTa]. The main idea in their construction is *localization.* Namely, use more precise information about local speed of wave propagation, in order to average the nonsmooth parts of the computed solution over smaller cells of variable size of order $O(\Delta t)$.

To construct the second-order KT schemes, we again reconstruct the piecewise-linear interpolant (7), $w(x, t^n)$, at time t^n based on the computed cell average $\bar{w}_j^n$. Before this interpolant is evolved in time, we estimate for the local speed of propagation at the center $x_{j+\frac{1}{2}}$ and denote the upper bound by $a^n_{j+\frac{1}{2}}$, i.e., the maximum speed of propagation. Moreover, denote

$$x^n_{j+\frac{1}{2},l} = x_{j+\frac{1}{2}} - \phi^n_{j+\frac{1}{2}}\Delta t; \quad x^n_{j+\frac{1}{2},r} = x_{j+\frac{1}{2}} + \phi^n_{j+\frac{1}{2}}\Delta t; \tag{11}$$

with a free parameter $\phi^n_{j+\frac{1}{2}}$ satisfying the CFL condition

$$a^n_{j+\frac{1}{2}} \leq \phi^n_{j+\frac{1}{2}} \leq \frac{1}{2\lambda}. \tag{12}$$

Due to finite speed of propagation, the points $x^n_{j+\frac{1}{2},l}, x^n_{j+\frac{1}{2},r}$ separate between smooth and possible singular regions $[x^n_{j-\frac{1}{2},r}, x^n_{j+\frac{1}{2},l}] \times [t^n, t^{n+1}]$ and $[x^n_{j+\frac{1}{2},l}, x^n_{j+\frac{1}{2},r}] \times [t^n, t^{n+1}]$. Under to the CFL restriction, (12), the required integrals of the fluxes in (3) over each anrrower rectangular controlled volumes can be approximated by the midpoint rule and the midpoint values, $w^{n+\frac{1}{2}}_{j+\frac{1}{2},l}$ and $w^{n+\frac{1}{2}}_{j+\frac{1}{2},r}$, can be obtained from the corresponding Taylor expansions with respect to $x^n_{j+\frac{1}{2},l}$ and $x^n_{j+\frac{1}{2},r}$, resulting with

$$\begin{aligned} &w^{n+1}_{j+\frac{1}{2}} \\ &= \frac{\bar{w}^n_j + \bar{w}^n_{j+1}}{2} + \frac{\Delta x - \phi^n_{j+\frac{1}{2}}\Delta t}{4}\left((w_x)_j - (w_x)_{j+1}\right) - \frac{1}{2\phi^n_{j+\frac{1}{2}}}\left[f(w^{n+\frac{1}{2}}_{j+\frac{1}{2},r}) - f(w^{n+\frac{1}{2}}_{j+\frac{1}{2},l})\right]; \end{aligned}$$

$$\begin{aligned} &w^{n+1}_j \\ &= \bar{w}^n_j + \frac{\Delta t}{2}\left(\phi^n_{j-\frac{1}{2}} - \phi^n_{j+\frac{1}{2}}\right)(w_x)_j - \frac{\lambda}{1 - \lambda(\phi^n_{j-\frac{1}{2}} - \phi^n_{j+\frac{1}{2}})}\left[f(w^{n+\frac{1}{2}}_{j+\frac{1}{2},l}) - f(w^{n+\frac{1}{2}}_{j-\frac{1}{2},r})\right]; \end{aligned}$$

$$w^{n+\frac{1}{2}}_{j+\frac{1}{2},l} := w^n_{j+\frac{1}{2},l} - \frac{\Delta t}{2} f(w^n_{j+\frac{1}{2},l})_x, \qquad w^n_{j+\frac{1}{2},l} := \bar{w}^n_j + (\frac{\Delta x}{2} - \phi^n_{j+\frac{1}{2}}\Delta t)(w_x)_j;$$
$$w^{n+\frac{1}{2}}_{j+\frac{1}{2},r} := w^n_{j+\frac{1}{2},r} - \frac{\Delta t}{2} f(w^n_{j+\frac{1}{2},r})_x, \qquad w^n_{j+\frac{1}{2},r} := \bar{w}^n_{j+1} - (\frac{\Delta x}{2} - \phi^n_{j+\frac{1}{2}}\Delta t)(u_x)_{j+1}.$$

To obtain the cell averages over the original grid of the uniform, non-staggered cells $[x_{j-\frac{1}{2}}, x_{j+\frac{1}{2}}]$, we consider the piecewise-linear construction at the time level t^{n+1}

$$w(x,t^{n+1}) := \sum_j \left\{ \left[w^{n+1}_{j+\frac{1}{2}} + (w_x)^{n+1}_{j+\frac{1}{2}}(x - x_{j+\frac{1}{2}}) \right] \chi_{[x^n_{j+\frac{1}{2},l}, x^n_{j+\frac{1}{2},r}]} + w^{n+1}_j \chi_{[x^n_{j-\frac{1}{2},r}, x^n_{j+\frac{1}{2},l}]} \right\}. \tag{13}$$

Here $\chi_{[x^n_{j+\frac{1}{2},l}, x^n_{j+\frac{1}{2},r}]}$ is the characteristic function on $[x^n_{j+\frac{1}{2},l}, x^n_{j+\frac{1}{2},r}]$ and the exact spatial derivatives, $w_x(x_{j+\frac{1}{2}}, t^{n+1})$, can be approximated by

$$(w_x)^{n+1}_{j+\frac{1}{2}} = \frac{2}{\Delta x} MM \left(\frac{w^{n+1}_{j+1} - w^{n+1}_{j+\frac{1}{2}}}{1 + \lambda(\phi^n_{j+\frac{1}{2}} - \phi^n_{j+\frac{3}{2}})}, \frac{w^{n+1}_{j+\frac{1}{2}} - w^{n+1}_j}{1 + \lambda(\phi^n_{j+\frac{1}{2}} - \phi^n_{j-\frac{1}{2}})} \right). \tag{14}$$

Finally, the desired cell averages, $\bar{w}^{n+1}_j$, are obtained by averaging the reconstructed approximate solution in (13) over the interval $[x_{j-\frac{1}{2}}, x_{j+\frac{1}{2}}]$, which leads to the final form of the second-order KT schemes

$$\begin{aligned} \bar{w}^{n+1}_j &= \lambda\phi^n_{j-\frac{1}{2}} w^{n+1}_{j-\frac{1}{2}} + \lambda\phi^n_{j+\frac{1}{2}} w^{n+1}_{j+\frac{1}{2}} + \left[1 - \lambda(\phi^n_{j+\frac{1}{2}} - \phi^n_{j-\frac{1}{2}})\right] w^{n+1}_j \\ &\quad + \frac{\Delta x}{2} \left[(\lambda\phi^n_{j-\frac{1}{2}})^2 (w_x)^{n+1}_{j-\frac{1}{2}} - (\lambda\phi^n_{j+\frac{1}{2}})^2 (w_x)^{n+1}_{j+\frac{1}{2}} \right]. \end{aligned}$$

3 New Schemes: Triangle version

We now demonstrate the construction of our new central-upwind scheme for nonlinear hyperbolic conservation laws (1). The main idea in the construction of our new central scheme is that instead of using a rectangular controlled volume determined by the local speed of wave propagation as in the construction of the KT scheme, we take a smaller triangular controlled volume which leads to less numerical viscosity when compared to the KT scheme. For simplicity, we demonstrate a second-order construction for one-dimensional case only. The construction may be extended to high-order or higher-dimensional cases. [KL]

As usual, assume that we have already computed the piecewise-linear solution, $w(x,t^n)$ and the local speed of wave propagation, $a^n_{j+\frac{1}{2}}$, at the time level t^n. We also choose two free parameters $\phi_{j+\frac{1}{2}}$ and $\epsilon > 0$ satisfying the CFL condition

$$a^n_{j+\frac{1}{2}} \le \phi^n_{j+\frac{1}{2}} \le \frac{1}{2\lambda} - \frac{\epsilon}{\Delta t}. \tag{15}$$

We then evolve this piecewise-linear interpolant in time and project at the next time level t^{n+1} onto two different kinds of regions: smooth and possible nonsmooth. In the possible non-smooth region, the interpolant is evolved in time starting from the interval $[x_{j+\frac{1}{2}} - \epsilon, x_{j+\frac{1}{2}} + \epsilon]$ and is projected onto the interval $[x^{n+1}_{j+\frac{1}{2},l} - \epsilon, x^{n+1}_{j+\frac{1}{2},r} + \epsilon]$ at the time level t^{n+1}. Here,

$$x^{n+1}_{j+\frac{1}{2},l} = x_{j+\frac{1}{2}} - \phi^n_{j+\frac{1}{2}}\Delta t; \quad x^{n+1}_{j+\frac{1}{2},r} = x_{j+\frac{1}{2}} + \phi^n_{j+\frac{1}{2}}\Delta t; \tag{16}$$

Exact computation of spatial integrals yield

$$\begin{aligned} w^{n+1}_{j+\frac{1}{2}} &:= \frac{1}{\Delta x_{j+\frac{1}{2}} + 2\epsilon} \int_{x^{n+1}_{j+\frac{1}{2},l}-\epsilon}^{x^{n+1}_{j+\frac{1}{2},r}+\epsilon} w(x, t^{n+1})dx \\ &= \frac{1}{\Delta x_{j+\frac{1}{2}} + 2\epsilon} \left[\int_{x_{j+\frac{1}{2}}-\epsilon}^{x_{j+\frac{1}{2}}+\epsilon} w(x, t^n)dx + \int_0^{\Delta t} w(y_{j+\frac{1}{2},r}(t), t)\phi^n_{j+\frac{1}{2}}dt + \int_0^{\Delta t} w(y_{j+\frac{1}{2},l}(t), t)\phi^n_{j+\frac{1}{2}}dt \right. \\ &\left. + \int_0^{\Delta t} f(w(y_{j+\frac{1}{2},l}(t), t))dt - \int_0^{\Delta t} f(w(y_{j+\frac{1}{2},r}(t), t))dt \right] \end{aligned} \tag{17}$$

Here $\Delta x_{j+\frac{1}{2}} := x^n_{j+\frac{1}{2},r} - x^n_{j+\frac{1}{2},l} = 2\phi^n_{j+\frac{1}{2}}\Delta t$. $y_{j+\frac{1}{2},r}(t) = x_{j+\frac{1}{2}} + \phi^n_{j+\frac{1}{2}}t + \epsilon$ and $y_{j+\frac{1}{2},l}(t) = x_{j+\frac{1}{2}} - \phi^n_{j+\frac{1}{2}}t - \epsilon$

Similarly, for the smooth parts, the interpolant is evolved in time starting from the interval $[x_{j-\frac{1}{2}} + \epsilon, x_{j+\frac{1}{2}} - \epsilon]$ and is projected onto the interval $[x^{n+1}_{j-\frac{1}{2},r} + \epsilon, x^{n+1}_{j+\frac{1}{2},l} - \epsilon]$ at time t^{n+1}, resulting in

$$\begin{aligned} w^{n+1}_{j} &:= \frac{1}{\Delta x_j - 2\epsilon} \int_{x^{n+1}_{j-\frac{1}{2},r}+\epsilon}^{x^{n+1}_{j+\frac{1}{2},l}-\epsilon} w(x, t^{n+1})dx \\ &= \frac{1}{\Delta x_j - 2\epsilon} \left[\int_{x_{j-\frac{1}{2}}+\epsilon}^{x_{j+\frac{1}{2}}-\epsilon} w(x, t^n)dx - \int_0^{\Delta t} w(y_{j+\frac{1}{2},l}(t), t)\phi^n_{j+\frac{1}{2}}dt + \int_0^{\Delta t} w(y_{j-\frac{1}{2},r}(t), t)\phi^n_{j-\frac{1}{2}}dt \right. \\ &\left. - \int_0^{\Delta t} f(w(y_{j+\frac{1}{2},l}(t), t))dt - \int_0^{\Delta t} f(w(y_{j-\frac{1}{2},r}(t), t))dt \right] \end{aligned} \tag{18}$$

where $\Delta x_j := x_{j+\frac{1}{2},l} - x_{j-\frac{1}{2},r} = \Delta x - (\phi^n_{j-\frac{1}{2}} + \phi^n_{j+\frac{1}{2}})\Delta t$.

Under the CFL restriction, (15), the required integrals in (17, 18) can be approximated by the midpoint rule and the midpoint values, $w^{n+\frac{1}{2}}_{j+\frac{1}{2},l}$ and $w^{n+\frac{1}{2}}_{j+\frac{1}{2},r}$, can be obtained from the corresponding Taylor expansions with respect to $x^n_{j+\frac{1}{2},l}$ and $x^n_{j+\frac{1}{2},r}$, resulting with (take $\epsilon \to 0$)

$$
\begin{aligned}
&w_{j+\frac{1}{2}}^{n+1} \\
&= \frac{\Delta t}{2\phi_{j+\frac{1}{2}}^n}\left[\left(w_{j+\frac{1}{2},r}^{n+\frac{1}{2}} + w_{j+\frac{1}{2},l}^{n+\frac{1}{2}}\right)\phi_{j+\frac{1}{2}}^n - f(w_{j+\frac{1}{2},r}^{n+\frac{1}{2}}) + f(w_{j+\frac{1}{2},l}^{n+\frac{1}{2}})\right];
\end{aligned}
$$

$$
w_j^{n+1} = \frac{\Delta t}{\Delta x_j}\left[(\Delta x)w_j^n - w_{j-\frac{1}{2},r}^{n+\frac{1}{2}}\phi_{j-\frac{1}{2}}^n - w_{j+\frac{1}{2},l}^{n+\frac{1}{2}}\phi_{j+\frac{1}{2}}^n - f(w_{j+\frac{1}{2},l}^{n+\frac{1}{2}}) + f(w_{j-\frac{1}{2},r}^{n+\frac{1}{2}})\right]; \tag{19}
$$

$$
w_{j+\frac{1}{2},l}^{n+\frac{1}{2}} := w_{j+\frac{1}{2},l}^n - \frac{\Delta t}{2}f(w_{j+\frac{1}{2},l}^n)_x, \qquad w_{j+\frac{1}{2},l}^n := \bar{w}_j^n + (\frac{\Delta x}{2} - \phi_{j+\frac{1}{2}}^n\Delta t)(w_x)_j;
$$

$$
w_{j+\frac{1}{2},r}^{n+\frac{1}{2}} := w_{j+\frac{1}{2},r}^n - \frac{\Delta t}{2}f(w_{j+\frac{1}{2},r}^n)_x, \qquad w_{j+\frac{1}{2},r}^n := \bar{w}_{j+1}^n - (\frac{\Delta x}{2} - \phi_{j+\frac{1}{2}}^n\Delta t)(w_x)_{j+1}.
$$

At this stage, we realize the solution at the time level t^{n+1} in terms of the approximate cell averages $w_{j+\frac{1}{2}}^{n+1}$ and w_j^{n+1}. To obtain the cell averages over the original grid of the uniform, non-staggered cells $[x_{j-\frac{1}{2}}, x_{j+\frac{1}{2}}]$, we consider the re-projection mechanism at time level t^{n+1} as proceeded in the construction of the KT schemes, (13, 14), and results in the final form of our second-order schemes

$$
\begin{aligned}
&\bar{w}_j^{n+1} \\
&= \frac{\phi_{j-\frac{1}{2}}^n\Delta t}{\Delta x}w_{j-\frac{1}{2}}^{n+1} + \frac{\phi_{j+\frac{1}{2}}^n\Delta t}{\Delta x}w_{j+\frac{1}{2}}^{n+1} + \left[1 - \lambda(\phi_{j+\frac{1}{2}}^n - \phi_{j-\frac{1}{2}}^n)\right]w_j^{n+1} \\
&\quad + \frac{1}{2\Delta x}\left[(\phi_{j-\frac{1}{2}}^n\Delta t)^2(w_x)_{j-\frac{1}{2}}^{n+1} - (\phi_{j+\frac{1}{2}}^n\Delta t)^2(w_x)_{j+\frac{1}{2}}^{n+1}\right].
\end{aligned}
$$

We end this section with three remarks

- Both KT and our schemes reduce to the NT scheme if we take $\phi_{j+\frac{1}{2}}^n = \frac{1}{2\lambda}$, hence to LxF schemes if we take furthermore, the numerical derivatives $(w_x)_{j+\frac{1}{2}}^{n+1} = 0 = (w_x)_j^n$.
- Both KT and our scheme enjoy the same semi-discrete formula when we take $\Delta t \to 0$. See [KL] for details.
- Numerical viscosity of our scheme is less than that of the KT scheme as it is designed to be so. Since the difference is quite small to see from most numerical simulation. However, this fact is confirmed numerically by Example 3 in the next section.

4 Numerical experiments

In this section, we present and compare numerical results via KT and our new schemes. In Example 1, we show the order test for our scheme. In Example 2, we show a standard test on the shock tube problem. Most numerical simulation by KT and our schemes are hard to distinguish each other. However, we present in Example 3 a sharper resolution of our scheme against the KT scheme.

Example 1. Burgers' equation.
Here, we solve the inviscid Burgers' equation

$$u_t + \left(\frac{u^2}{2}\right)_x = 0, \qquad -1 \le x \le 1, \tag{20}$$

subject to the 2-periodic initial data $u_0(x) = 0.25+0.5\sin(\pi x)$. Table 1 shows the error and second-order order of our schemes at time $T = 1.5$, before the shock develops.

Table 1. Error and order in L_1 norm

	CFL = .45		CFL = .25	
No	L1 norm	L1 order	L1 norm	L1 order
40	0.002070	1.857520	0.002834	1.890214
80	0.000548	1.916432	0.000735	1.947920
160	0.000145	1.922300	0.000194	1.918088
320	0.000039	1.900322	0.000051	1.919836
640	0.000010	1.926276	0.000013	1.937500

Example 2. 1D Shock tube problem.
In this example, we apply our schemes to the 1D shock tube problem governed by the Euler system, where

$$\begin{aligned} u &= (\rho, \rho u, E)^T, \\ f(u) &= (\rho u, P + \rho u^2, u(E+P))^T, \end{aligned} \tag{21}$$

augmented with $P = (\gamma - 1)(E - \frac{1}{2}\rho u^2)$. Here ρ, u, P and E are respectively, the density, velocity, pressure and total specific energy. The system is complete with Sod's initial data

$$(\rho_L, u_L, P_L) = (1, 0, 1), x < 0 \qquad (\rho_R, u_R, P_R) = (0.125, 0, 0.1), x > 0.$$

In Figure 1, we show the density, velocity and pressure plots obtained by our schemes.

Example 3. Steady contact discontinuity.
We solve the 1D Euler system (21) on the interval $[-0.2, 0.2]$, subject to the initial data

$$\mathbf{u}(x,0) = \begin{cases} \mathbf{u}_L = (1, 0, 2.5)^T, & x < 0, \\ \mathbf{u}_R = (0.5, 0, 2.5)^T, & x > 0, \end{cases} \tag{22}$$

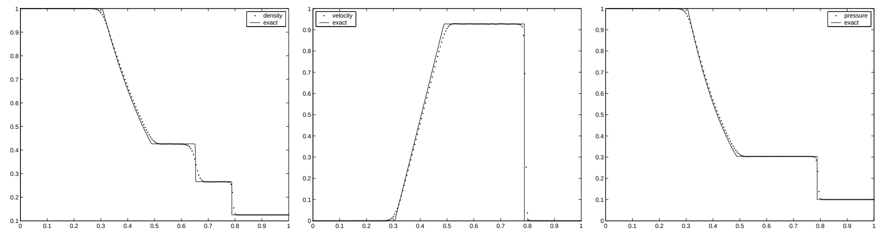

Fig. 1. Shock tube problem: Sod's initial data

which corresponds to a single steady contact discontinuity. We use 80 grid points and compute the solution at a final time $T = 10$. Figure 2 shows the density, computed using the KT and our new schemes. The excessive numerical viscosity, present in all these schemes, does not allow a sharp resolution of the discontinuity. However, our scheme gives a better resolution of the steady contact wave.

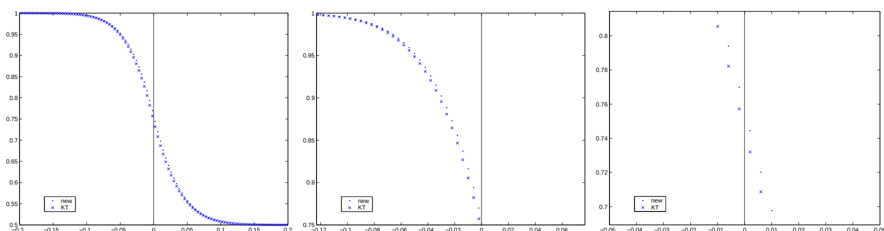

Fig. 2. Steady contact discontinuity

References

[JLLOT] Jiang, G.-S., Levy, D., Lin,C.-T., Osher, O., Tadmor, E., (1998): High-Resolution Non-Oscillatory Central Schemes with Non-Staggered Grids for Hyperbolic Conservation Laws. SIAM J. Numer. Anal.,

[KL] Kurganov, A., Lin, C.-T., (2003): On the Reduction of Numerical Dissipation in Central-Upwind Schemes. In preparation.

[KurTa] Kurganov, A., Tadmor, E., (2000): New High-Resolution Central Schemes for Nonlinear Conservation Laws and Convection-Diffusion Equations. JCP, **160**, 241–282.

[NeTa] Nessyahu, H., Tadmor, E., (1990): Non-oscillatory Central Differencing for Hyperbolic Conservation Laws. JCP, **87**, 408–463.

[LeVe] LeVeque, R. (2002): Finite Volume methods for Hyperbolic Problems. Cambridge University Press.